ELSEVIER

Journal of Alloys and Compounds 343 (2002) 204–210

Journal of ALLOYS AND COMPOUNDS

www.elsevier.com/locate/jallcom

Growth of $LiCaAlF_6$ single crystals with an extended diameter and their optical characterizations

Kiyoshi Shimamura[a,*], Hiroki Sato[b], Amina Bensalah[a], Hiroshi Machida[b], Nobuhiko Sarukura[c], Tsuguo Fukuda[a]

[a]*Institute for Materials Research, Tohoku University, Sendai 980-8577, Japan*
[b]*Tokin Corporation, Saitama 360-0843, Japan*
[c]*Institute for Molecular Science, Okazaki 444-8585, Japan*

Received 3 January 2002; accepted 28 January 2002

Abstract

$LiCaAlF_6$ (LiCAF) single crystals with an extended diameter were grown by the Czochralski (CZ) technique under CF_4 atmosphere. Modifying the growth conditions enabled the growth of LiCAF single crystals with 3- and 4-inch diameters. After considering reflection loss, LiCAF showed transmittance over 95% at 157 nm. A precise measurement of the refractive index showed that the birefringence of LiCAF vanished at around 152 nm. The fabrication of a LiCAF lens was demonstrated.

Keywords: Optical materials; Crystal growth; Optical properties

1. Introduction

Much of the tremendous progress in integrated circuit technology and performance over the past 30 years has been fueled by the progress in lithography [1]. The ability to print increasingly smaller features has enabled higher speed transistors, higher packing densities and lower power dissipation in CMOS circuits [2]. In pursuit of ever smaller feature sizes it has been necessary for the semiconductor industry to move from mercury UV lamps operating at the g-line wavelength, to i-line and more recently to the shorter wavelength pulsed 248 nm light available from KrF filled excimer lasers. Steppers utilizing 193 nm light from ArF filled excimer lasers are now being introduced and SEMATECH, a forum comprised of the major silicon device manufacturers world-wide, has designated 157 nm as the route to realize device structures of 100 nm and below [3]. A very bright source for this wavelength is the molecular fluorine laser, often misleadingly referred to as an excimer laser because with a suitable change of optics and gas mix it operates in the same device as rare gas halide lasers [4,5]. One of the most serious problems in realizing a 157-nm based system is the development of suitable optical materials for lenses and other optical components. Although 248- and 193-nm based systems could be realized using fused silica and CaF_2, a new material is required for 157-nm based systems because of the limitation of fused silica transparency. In fact, a 2-mm-thick UV-grade fused silica plate transmits less than 10% at 157 nm [6]. In particular, for an all-refractive design 157 nm laser source, a second material other than CaF_2 is strongly required. Primary candidates for a second material were LiF and MgF_2; however, they have several disadvantages such as a fragile and hygroscopic nature and large birefringence [7].

Other than the above binary fluorides, complex fluoride single crystals, such as Colquiriite- and Perovskite-type fluorides, also present many advantages as optical materials, because of their unique properties, such as a large band gap. However, detailed characteristics of the complex fluoride single crystals have not yet been investigated well, mainly because the growth of these crystals is known to be difficult. For the growth of these crystals, a fluorination process using gases such as HF [8] is usually performed in order to purify both the raw materials and the growing crystals. We previously reported the growth of Ce:LiCAF

*Corresponding author. Present address: Kugami Memorial Laboratory for Materials Science and Technology, Waseda University, 2-8-26 Nishiwaseda, Shinjuku, Tokyo 169-0051, Japan. Tel.: +81-3-5286-3793; fax: +81-3-5286-3793.

E-mail address: shimak@waseda.jp (K. Shimamura).

0925-8388/02/$ – see front matter
PII: S0925-8388(02)00125-1

crystals without either the use of HF gases or the hydrofluorination of raw materials [9].

In the present work, we describe the growth of LiCAF single crystals with an extended diameter by the Czochralski (CZ) technique under modified growth conditions based on the investigations reported in Refs. [9–12]. Since grown crystals have shown superior transmission in the UV and vacuum-ultra-violet (VUV) wavelength region, the promising application of them as window materials for optical lithography is also discussed, identifying them as a new, promising material.

2. Experiment

Crystal growth was performed in a CZ system with a resistive heater made of high-purity graphite. The starting material was prepared from commercially available LiF, CaF_2 and AlF_3 powders of high purity (>99.99%). The starting material was placed in a Pt crucible. Vacuum treatment was performed prior to growth. The system was heated from room temperature to 700 °C for a period of 12 h under vacuum ($\approx 10^{-3}$ Pa). Both rotary and diffusion pumps were used to achieve $\approx 10^{-3}$ Pa and effectively eliminate water and oxygen from the growth chamber and the starting material. Subsequently, high purity CF_4 gas (99.99%) was slowly introduced into the furnace. Thereafter, the starting material was melted at approximately 820 °C. Transmission in the VUV wavelength region at room temperature was analyzed by VUV 5530 spectrophotometry under vacuum. LiCAF wafers with a thickness of 2.0 mm for this analysis were fabricated by cutting grown crystals pulled at a rate of 0.8 mm/h and polishing them. The refractive index of the LiCAF crystals was measured accurately down to five decimal places. The LiCAF crystal was cut in the shape of a dispersion prism, 60 degrees and 20 mm on each side and polished. The measurement was performed at 27 different wavelengths from 148 to 656 nm with the minimum deviation method. The refractive indices were measured for different polarized light parallel and vertical to the *c* axis of the crystal, (n_e, n_o). The measurement was performed under N_2 atmosphere and the temperature was controlled between 24.9 and 25.0 °C.

3. Results and discussion

The growth of LiCAF single crystals with a 3-inch diameter was investigated. Powdered raw materials were placed in a 130-mm diameter crucible. As the vaporization from melt was thought to be increased because of the extended melt surface area, the starting melt composition was prepared in more LiF and AlF_3 enriched directions (10%-rich, respectively). Crystals were grown at a pulling and rotation speed of 0.8 mm/h and 8 rpm, respectively. Fig. 1 shows a 3-inch diameter LiCAF crystal with inclusions. Although the diameter of the grown crystal was controlled precisely, the formation of inclusions could not be avoided. This means that the precise control of the diameter is not sufficient for the growth of 3-inch diameter LiCAF, while it was effective for the growth of 2-inch diameter LiCAF to avoid inclusions [13]. Further, the preparation of the starting melt composition in more LiF and AlF_3 enriched directions was also not sufficient. One

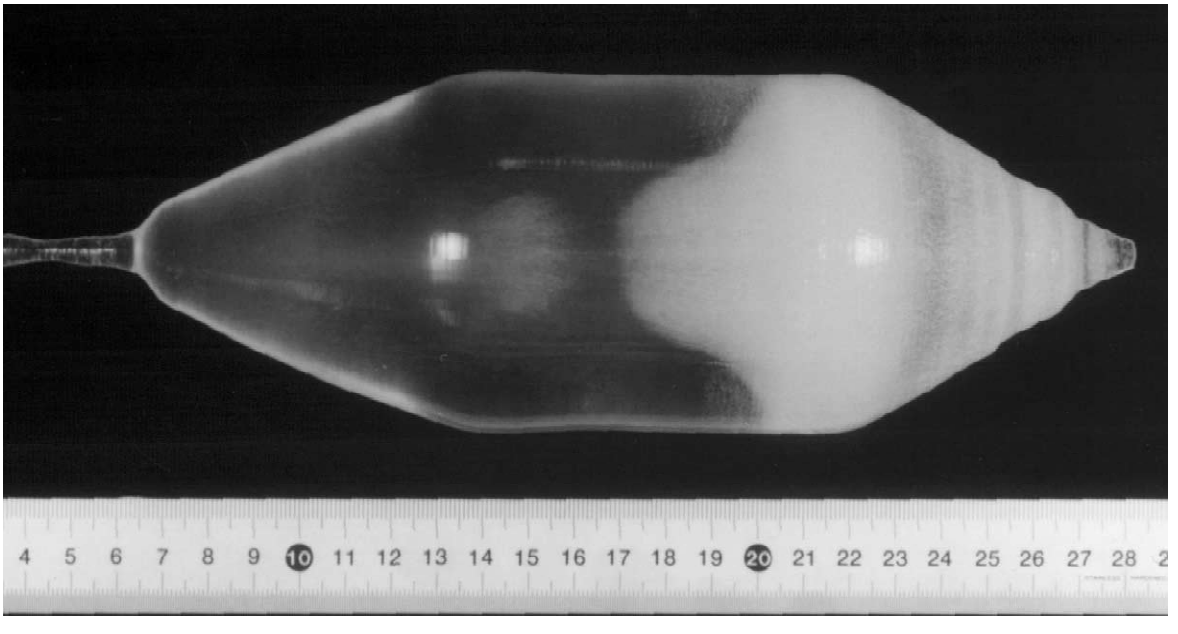

Fig. 1. $LiCaAlF_6$ crystal 3 inches in diameter with inclusions.

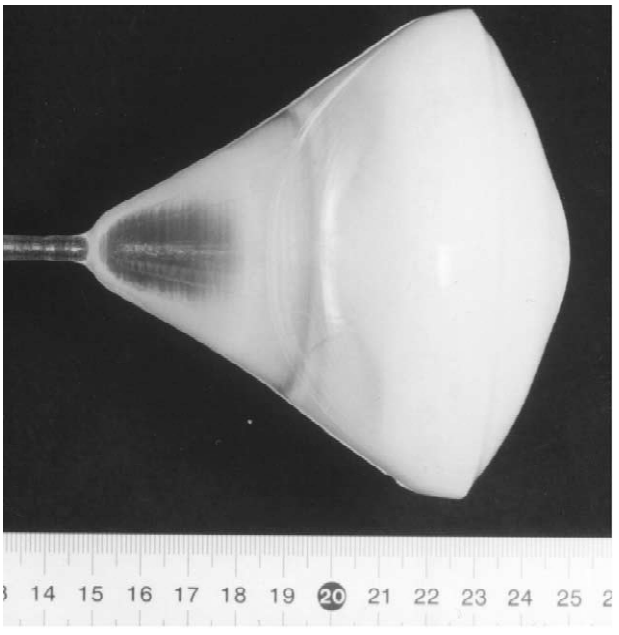

Fig. 2. $LiCaAlF_6$ crystal separated from the melt compulsorily.

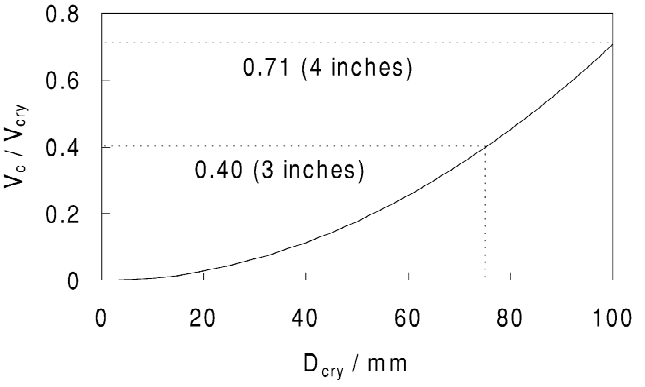

Fig. 3. Raising speed of a crucible depending on the diameter of the grown crystal.

of the possible reasons for the formation of inclusions is the instability of the growth interface between the melt and crystal. Fig. 2 also shows a crystal separated from the melt compulsorily, in order to see the growth interface. As can be seen, the growth interface is fairly convex toward the melt, and it has a relatively unstable shape, indicating the instability of crystal growth. One way to improve this instability is to increase the crystal rotation rate. Another possible reason for the formation of inclusions is the descent of the melt level. Since the volume of the melt for the growth of 3-inch LiCAF single crystals is larger than that for 1- or 2-inch crystals, the descent of the melt level is also larger. When the melt level changes drastically, the temperature condition around the growth interface also changes drastically. One way to keep it constant is to raise the crucible with the growth of a crystal. The raising speed of the crucible to maintain a constant melt level can be calculated using the diameter of the crucible and the grown crystal. Since the weight of melt spent for crystal growth and that of a grown crystal are equal, it can be calculated by the following relation:

$$\pi(D_c/2)^2 V_c d_{liq} = \pi(D_{cry}/2)^2 V_{cry} d_{cry}, \quad (1)$$

where D_c, D_{cry}, V_c, V_{cry}, d_{liq} and d_{cry} are the diameter of a crucible, that of the crystal grown, the raising speed of a crucible, crystal growth speed, the density of the melt, and that of the crystal grown, respectively. Fig. 3 shows the raising speed of the crucible, calculated from Eq. (1). The speed increases along a curve plotted as function of the increase of the diameter of the grown crystal. At a crystal diameter of 75 mm, the raising speed of the crucible is 0.32 mm/h when the growth speed of the crystal is 0.8 mm/h, since the ratio V_c/V_{cry} is approximately 0.40. Fig. 4 shows a LiCAF crystal grown by modifying the crystal rotation rate from 8 rpm to 12 rpm, and by raising the crucible continuously. The formation of inclusions was not observed, while many cracks appeared in a grown crystal. This is probably due to the occurrence of thermal stress in a grown crystal, since the grown crystal was located at a position where the temperature gradient was high during the cooling process. Especially, more cracks were observed at the shoulder part of the grown crystal. This is because the temperature gradient of the upper part inside the furnace was larger. With crystals grown with a fixed crucible position, the formation of cracks was not observed. When the crucible was not raised, the distance to be pulled up could not be relatively large, because crystals were grown toward the crucible bottom with the distance corresponding to the descent of the melt level. Therefore, grown crystals could not be pulled up to the position where the temperature gradient was large. Based on this consideration, the grown crystal and the crucible were lowered to their positions after the crystal growth process, and the grown crystal was cooled at the position where temperature gradient was lower, in order to avoid crack formation. Fig. 5 shows a LiCAF single crystal of 3 inches in diameter, free from cracks and inclusions. The surface of the shoulder part displayed a slight adherance of vaporized white material composed of LiF and AlF_3 during crystal growth, while the crystal itself was transparent. Based on the above results, a LiCAF single crystal with a 4-inch diameter was grown (Fig. 6).

Fig. 7 shows the transmission spectra of the grown LiCAF single crystals. Reflection loss of the surface of LiCAF crystals was also measured in order to estimate the absolute transmittance. Fig. 7 also shows the reflection from the surface of the crystals. It is shown that the reflection rapidly increases around 140 nm and the mag-

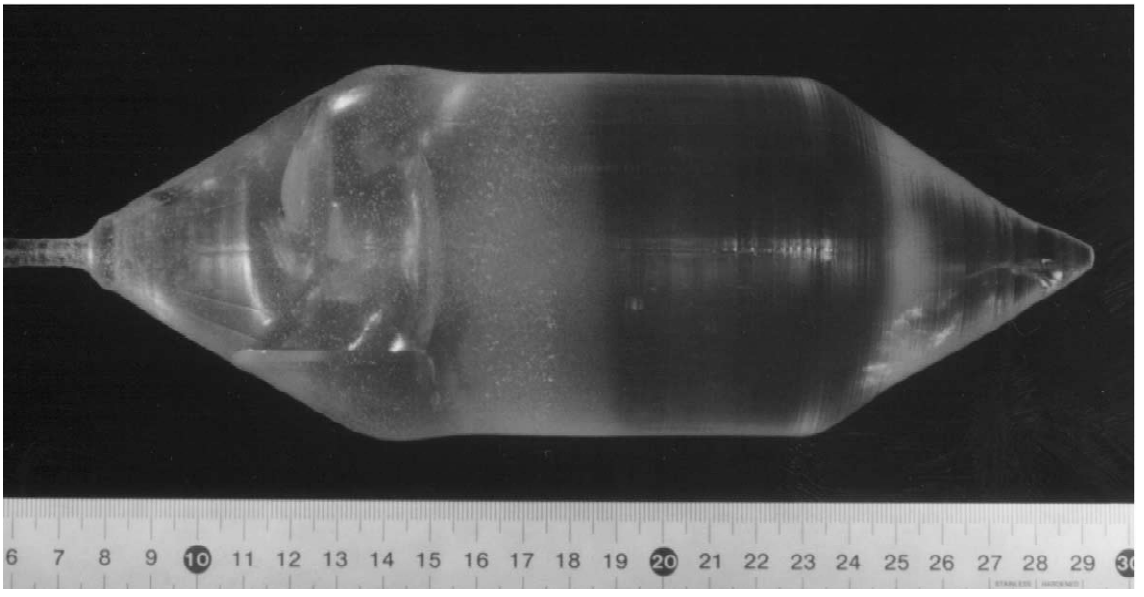

Fig. 4. As-grown $LiCaAlF_6$ crystal 3 inches in diameter with cracks.

nitude of the reflection is fairly high. This is a problem of commonly used optical materials in the UV and VUV wavelength regions. The transmittance is usually defined by the following equation:

$$T = \frac{I}{I_0}, \tag{2}$$

where I_0 is the incident ray, I is the transmitted ray, respectively. If reflection or scattering of the surface is not taken into consideration, the transmittance can also be shown to obey the following equation (Lambert's law):

$$T = \frac{I}{I_0} = \mathrm{e}^{-\alpha t}. \tag{3}$$

In a practical measurement, reflection from two surfaces of the crystal sample should be considered. If reflection

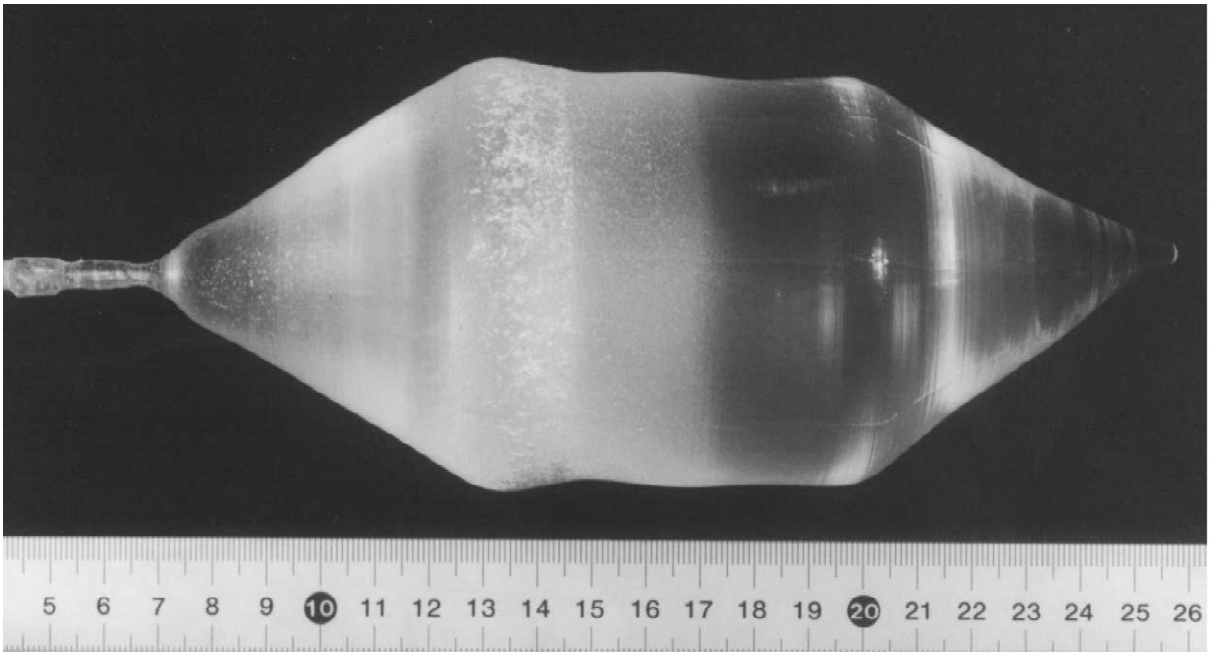

Fig. 5. As-grown $LiCaAlF_6$ single crystal 3 inches in diameter, free from inclusions and cracks.

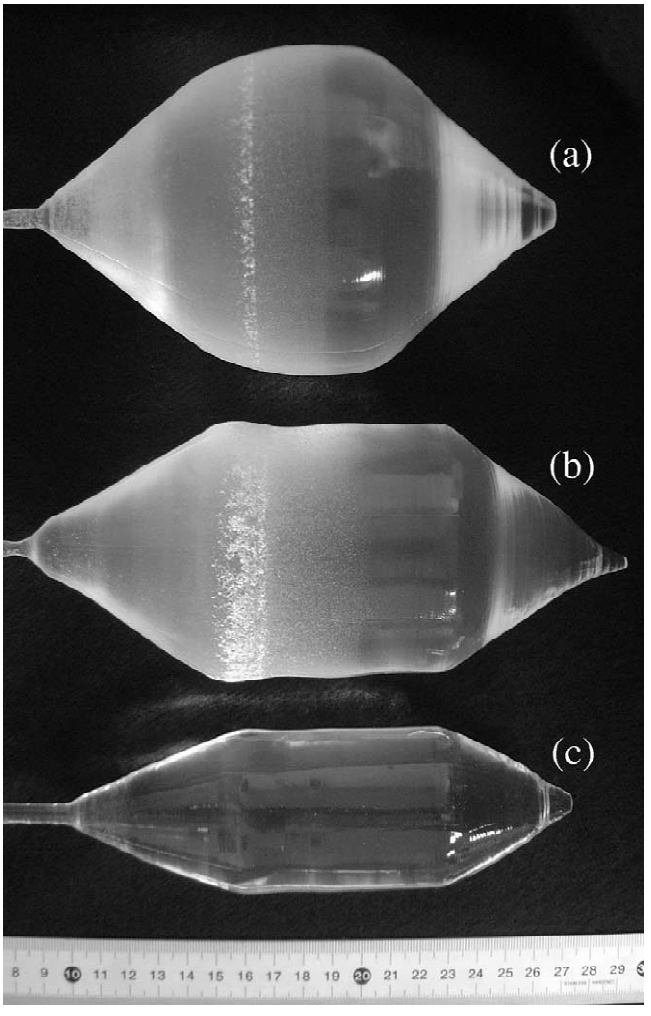

Fig. 6. As-grown $LiCaAlF_6$ single crystal 4 inches (a), 3 inches (b), and 2 inches (c) in diameter, respectively.

occurs as a multiple reflection in the crystal, it can be derived from Eq. (3) using the absorption coefficient calculated from Eq. (2) [14]:

$$T = \frac{(1-R)^2 \, e^{-\alpha t}}{1 - R^2 \, e^{-2\alpha t}}, \tag{4}$$

where α is the absorption coefficient and t is the thickness of sample, respectively. T as defined by this equation is often called external transmittance. After considering reflection loss, a higher transmittance could be obtained (Fig. 7). It should be noticed that LiCAF showed a transmittance of over 95% at 157 nm, which corresponds to the wavelength of an F_2 laser.

Fig. 8 shows a prism prepared for the measurement of refractive indices, and Table 1 shows the measured refractive indices. The coefficients of Sellmeier's equation (as shown below) for LiCAF crystals were calculated from 27 measured refractive indices by the least square method. Table 2 shows the coefficients calculated from the Sellmeier equation for LiCAF single crystals.

$$n^2 = A_0 + A_1\lambda^2 + A_2\lambda^{-2} + A_3\lambda^{-4} + A_4\lambda^{-6} + A_5\lambda^{-8} + A_6\lambda^{-10}. \tag{5}$$

Fig. 9 shows refractive indices measured depending on wavelength, together with lines calculated from the Sellmeier equation for LiCAF, Eq. (5). The results show that the indices increase for shorter wavelengths in positive dispersion and that the difference of refractive indices between n_e and n_o, birefringence, is very small, about 0.001. Especially, it was estimated by Eq. (5) that n_e and n_o could have exactly the same value at around 152 nm, which corresponds to the disappearance of birefringence in the LiCAF crystals.

In order to investigate the possibility of fabricating optical devices, lens processing using LiCAF single crystals was examined. Fig. 10 shows a lens as an example,

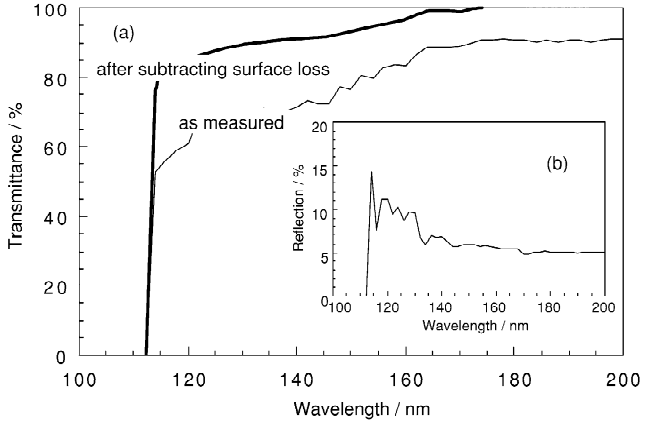

Fig. 7. Transmission spectra of $LiCaAlF_6$ crystal wafer with a thickness of 2.0 mm (a), and reflection from the surface of the same $LiCaAlF_6$ crystal wafer (b).

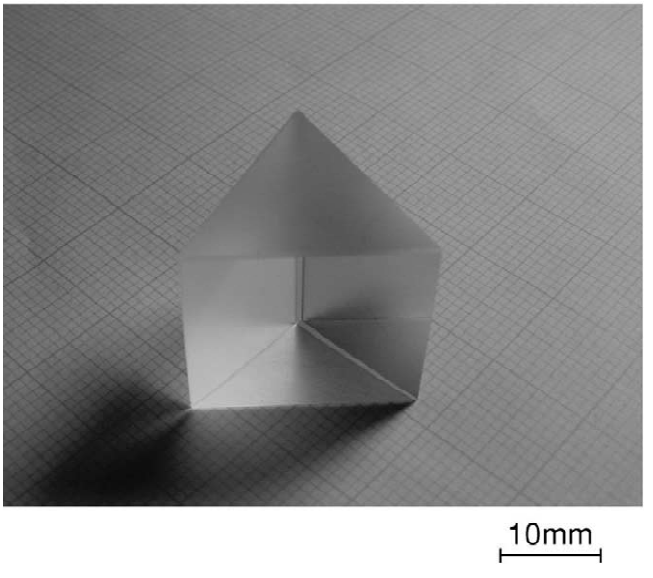

Fig. 8. $LiCaAlF_6$ prism prepared for the precise measurements of refractive indices.

Table 1
Refractive indices of a LiCAF single crystal measured depending on wavelength

Wavelength / nm	n_e	n_o
656.454	1.38473	1.38594
632.990	1.38508	1.38630
587.725	1.38587	1.38708
546.227	1.38674	1.38796
480.126	1.38860	1.38981
435.957	1.39033	1.39154
404.770	1.39191	1.39310
365.119	1.39454	1.39572
334.244	1.39732	1.39849
312.657	1.39980	1.40095
296.814	1.40202	1.40316
253.728	1.41062	1.41168
228.872	1.41837	1.41937
214.506	1.42443	1.41937
202.613	1.43074	1.43161
194.227	1.43612	1.43693
184.950	1.44326	1.44398
180.2940	1.44744	1.44811
177.7087	1.44996	1.45059
175.3829	1.45237	1.45297
172.3131	1.45578	1.45631
166.9231	1.46243	1.46287
162.1659	1.46917	1.46950
157.4306	1.47688	1.47708
155.2327	1.48086	1.48098
149.9371	1.49171	1.49163
148.2826	1.49554	1.49537

Table 2
Calculated coefficients from the Sellmeier equation for $LiCaAlF_6$ single crystals

	n_e	n_e
A_0	1.908116	1.911699
A_1	−4.0285616E−03	−4.366289E−03
A_2	4.720407E−03	4.686344E−03
A_3	2.644173E−05	2.735472E−05
A_4	7.129165E−07	6.291340E−07
A_5	−9.573848E−09	−7.916701E−09
A_6	1.701928E−10	1.515689E−10

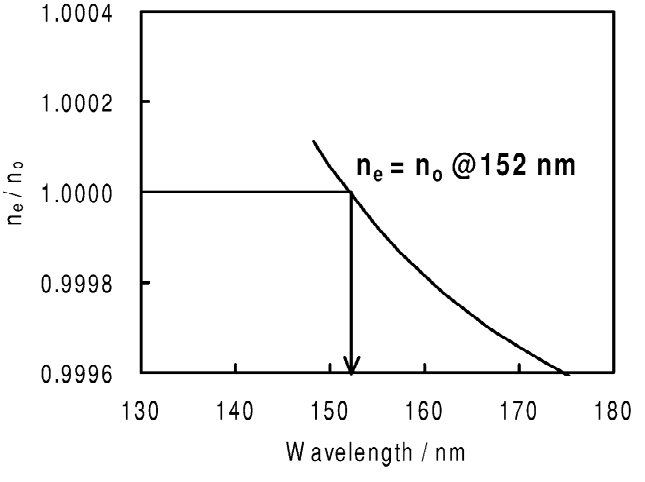

Fig. 9. Refractive indices of the $LiCaAlF_6$ single crystal depending on wavelength.

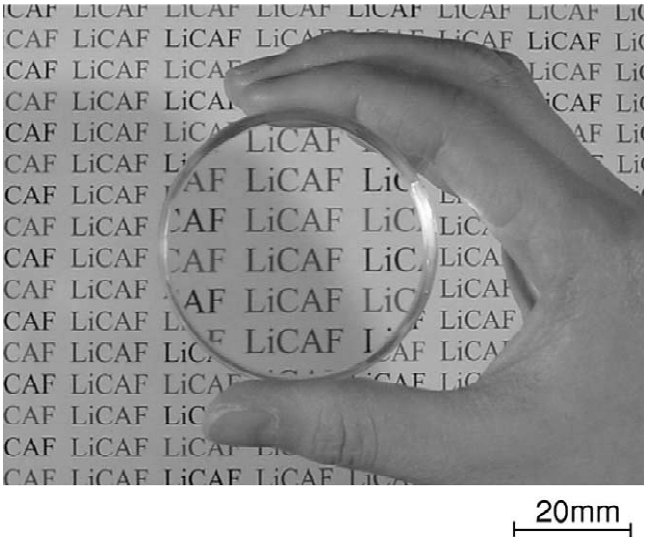

Fig. 10. A $LiCaAlF_6$ lens with one side spherically polished.

with one side spherically polished. This shows that LiCAF displays stability for processing such as cutting and polishing.

4. Summary

In this work, by modifying the crystal growth conditions, such as increasing the rotation speed, raising the crucible position to maintain a constant melt level, and cooling a grown crystal at a position with a lower temperature gradient, LiCAF single crystals 100 mm (4 inches) in diameter were grown. Using these grown LiCAF single crystals, the fabrication of one side of a spherically polished lens was demonstrated. This shows the stability of LiCAF for processing. Furthermore, precise measurement of the refractive index for LiCAF shows that birefringence disappears around 152 nm. Since this wavelength is very close to that of an F_2 laser, this birefringence disappearance makes the use of LiCAF for F_2 laser sources, more favourable.

References

[1] The National Technology Roadmap for Semiconductors. Semiconductor Industry Association.
[2] L.R. Harriott, Mater. Sci. Semicond. Process. 1 (1998) 93.
[3] R. Harbison, in: Proceedings of the First International Symposium on 157 nm Lithography, Dana Point, CA, USA, Vol. 1, 2000, pp. 9–33.
[4] S.M. Hooker, P.T. Landsberg, Progress in Quantum Electronics 18 (1994) 227.
[5] M.D. Whitfield, S.P. Lansley, O. Gaudin, R.D. McKeag, N. Rizvi, R.B. Jackman, Diam. Relat. Mater. 10 (2001) 693.
[6] T.M. Bloomstein, V. Liberman, M. Rothschild, D.E. Hardy, R.B. Goodman, Proc. Emerg. Lithogr. Technol. III, SPIE 3676 (1999) 342.

[7] T.M. Bloomstein, M.W. Hom, M. Rothschild, R.R. Kunz, S.T. Palmacol, R.B. Goodman, J. Vac. Sci. Technol. B 15 (1997) 2112.
[8] R.F. Belt, R. Uhrin, J. Cryst. Growth 109 (1991) 340.
[9] K. Shimamura, N. Mujilatu, K. Nakano, S.L. Baldochi, Z. Liu, H. Ohtake, N. Sarukura, T. Fukuda, J. Cryst. Growth 197 (1999) 896.
[10] S.L. Baldochi, K. Shimamura, K. Nakano, N. Mujilatu, T. Fukuda, J. Cryst. Growth 200 (1999) 521.
[11] S.L. Baldochi, K. Shimamura, K. Nakano, N. Mujilatu, T. Fukuda, J. Cryst. Growth 205 (1999) 537.
[12] K. Shimamura, S.L. Baldochi, N. Mujilatu, K. Nakano, Z. Liu, N. Sarukura, T. Fukuda, J. Cryst. Growth 211 (2000) 302.
[13] K. Shimamura, S.L. Baldochi, I.M. Marcia, H. Sato, T. Fujita, V.L. Mazzocchi, C.B.R. Parente, C.O. Paiva-Santos, C.V. Santilli, N. Sarukura, T. Fukuda, J. Cryst. Growth 223 (2001) 383.
[14] A. Ohsawa, K. Honda, S. Ohkawa, R. Ueda, Appl. Phys. Lett. 36 (1980) 147.